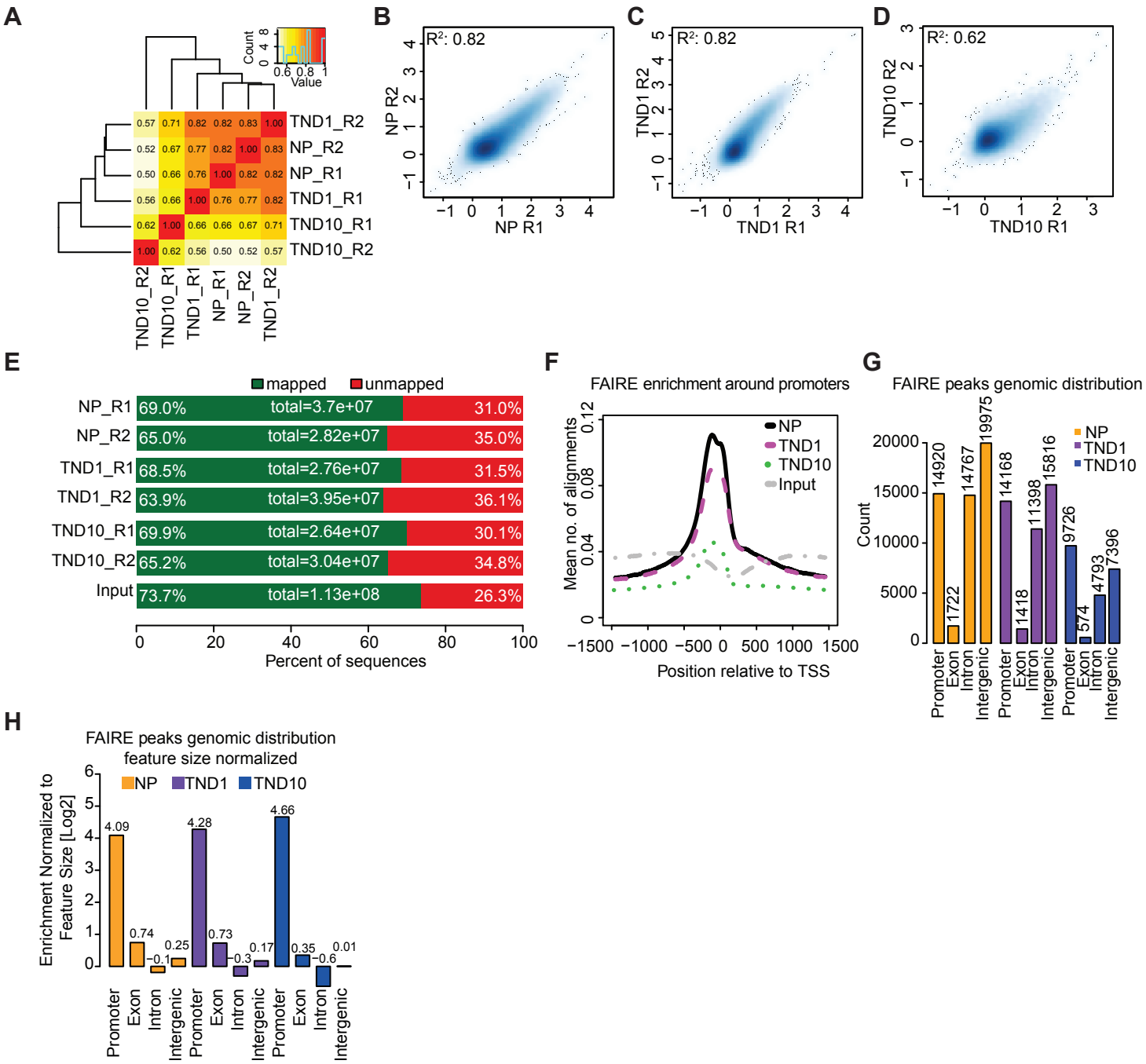
A
Count
Value
TND1_R2
NP_R2
NP_R1
TND1_R1
TND10_R1
TND10_R2
B
R²: 0.82
NP R2
NP R1
C
R²: 0.82
TND1 R2
TND1 R1
D
R²: 0.62
TND10 R2
TND10 R1
E
mapped
unmapped
NP_R1 69.0% total=3.7e+07 31.0%
NP_R2 65.0% total=2.82e+07 35.0%
TND1_R1 68.5% total=2.76e+07 31.5%
TND1_R2 63.9% total=3.95e+07 36.1%
TND10_R1 69.9% total=2.64e+07 30.1%
TND10_R2 65.2% total=3.04e+07 34.8%
Input 73.7% total=1.13e+08 26.3%
Percent of sequences
F
FAIRE enrichment around promoters
Mean no. of alignments
NP
TND1
TND10
Input
Position relative to TSS
G
FAIRE peaks genomic distribution
Count
NP
TND1
TND10
14920
1722
14767
19975
14168
1418
11398
15816
9726
574
4793
7396
Promoter
Exon
Intron
Intergenic
H
FAIRE peaks genomic distribution
feature size normalized
Enrichment Normalized to Feature Size [Log2]
NP
TND1
TND10
4.09
0.74
−0.1
0.25
4.28
0.73
−0.3
0.17
4.66
0.35
−0.6
0.01
Promoter
Exon
Intron
Intergenic

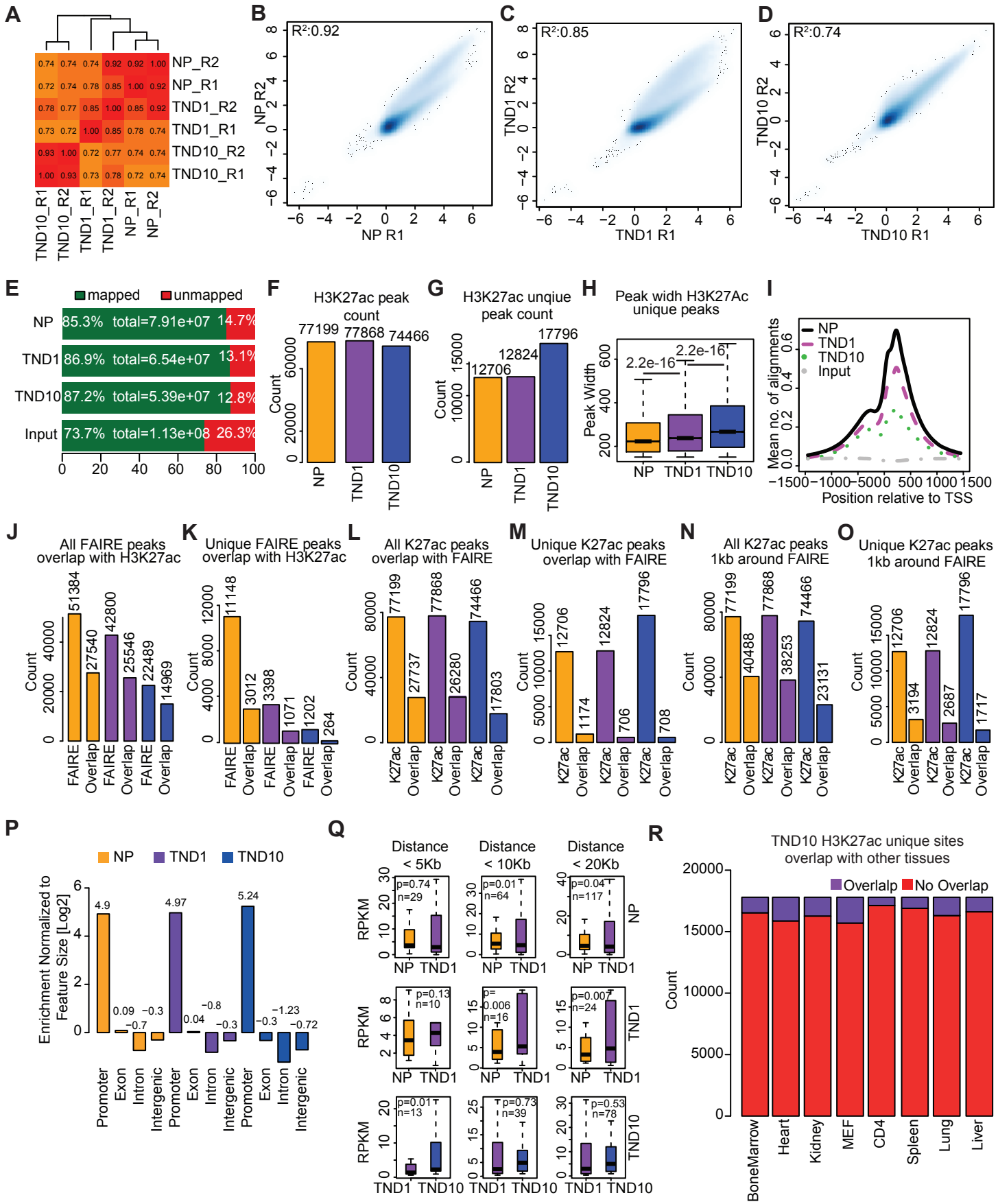
A
NP_R2
NP_R1
TND1_R2
TND1_R1
TND10_R2
TND10_R1
B
R²:0.92
NP R2
NP R1
C
R²:0.85
TND1 R2
TND1 R1
D
R²:0.74
TND10 R2
TND10 R1
E
mapped
unmapped
NP 85.3% total=7.91e+07 14.7%
TND1 86.9% total=6.54e+07 13.1%
TND10 87.2% total=5.39e+07 12.8%
Input 73.7% total=1.13e+08 26.3%
F
H3K27ac peak count
77199 77868 74466
Count
G
H3K27ac unqiue peak count
12706 12824 17796
H
Peak widh H3K27Ac unique peaks
2.2e-16
2.2e-16
Peak Width
I
NP
TND1
TND10
Input
Mean no. of alignments
Position relative to TSS
J
All FAIRE peaks overlap with H3K27ac
51384 27540 42800 25546 22489 14969
K
Unique FAIRE peaks overlap with H3K27ac
11148 3012 3398 1071 1202 264
L
All K27ac peaks overlap with FAIRE
77199 27737 77868 26280 74466 17803
M
Unique K27ac peaks overlap with FAIRE
12706 1174 12824 706 17796 708
N
All K27ac peaks 1kb around FAIRE
77199 40488 77868 38253 74466 23131
O
Unique K27ac peaks 1kb around FAIRE
12706 3194 12824 2687 17796 1717
P
NP
TND1
TND10
Enrichment Normalized to Feature Size [Log2]
4.9 0.09 −0.7 −0.3 4.97 0.04 −0.8 −0.3 5.24 −0.3 −1.23 −0.72
Promoter Exon Intron Intergenic
Q
Distance < 5Kb
Distance < 10Kb
Distance < 20Kb
RPKM
p=0.74 n=29
p=0.01 n=64
p=0.04 n=117
p=0.13 n=10
p= 0.006 n=16
p=0.007 n=24
p=0.01 n=13
p=0.73 n=39
p=0.53 n=78
R
TND10 H3K27ac unique sites overlap with other tissues
Overlalp
No Overlap
Count
BoneMarrow Heart Kidney MEF CD4 Spleen Lung Liver

Supplemental Figure S3 **Thakurela & Sahu et al.**

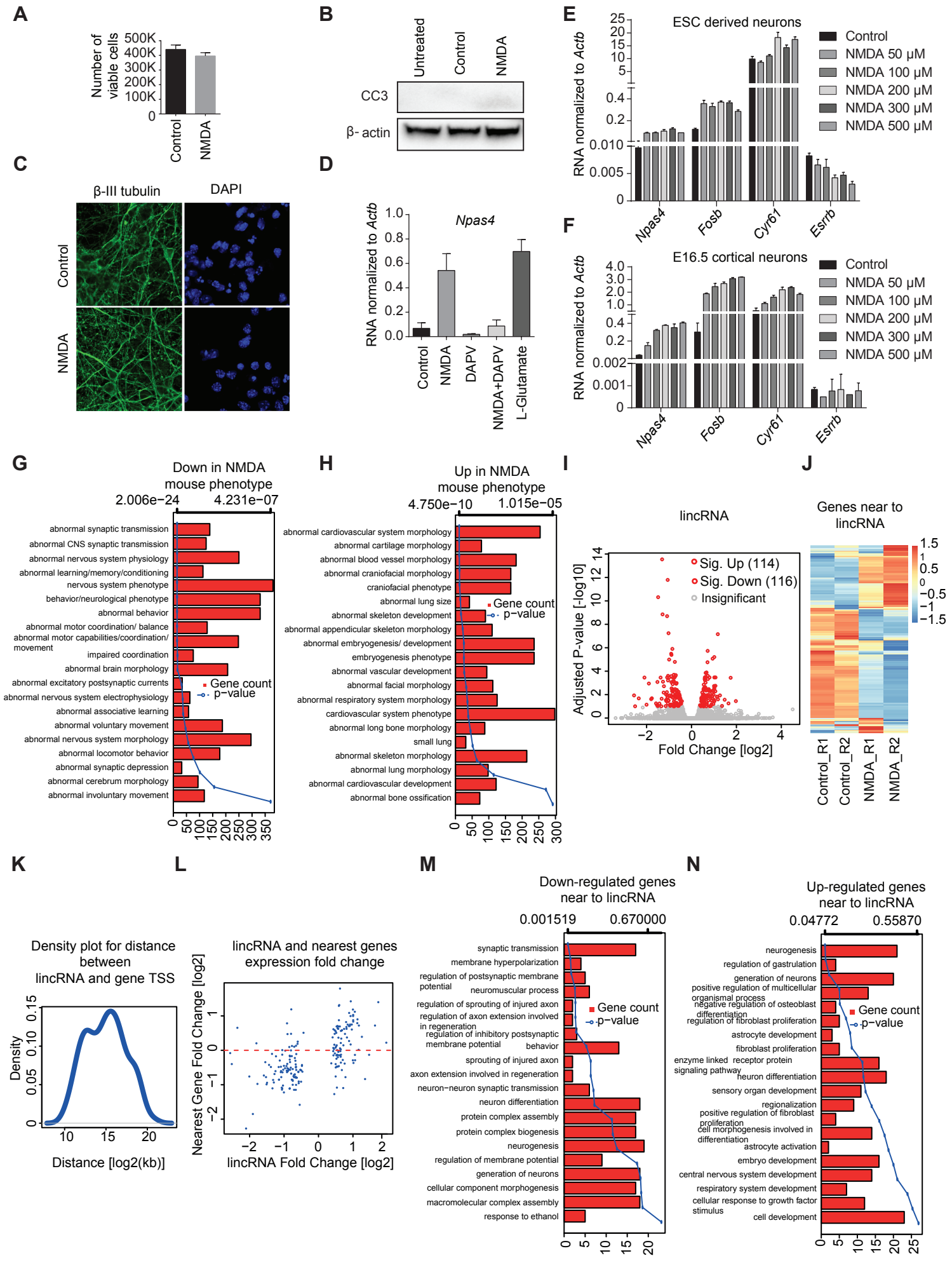

A

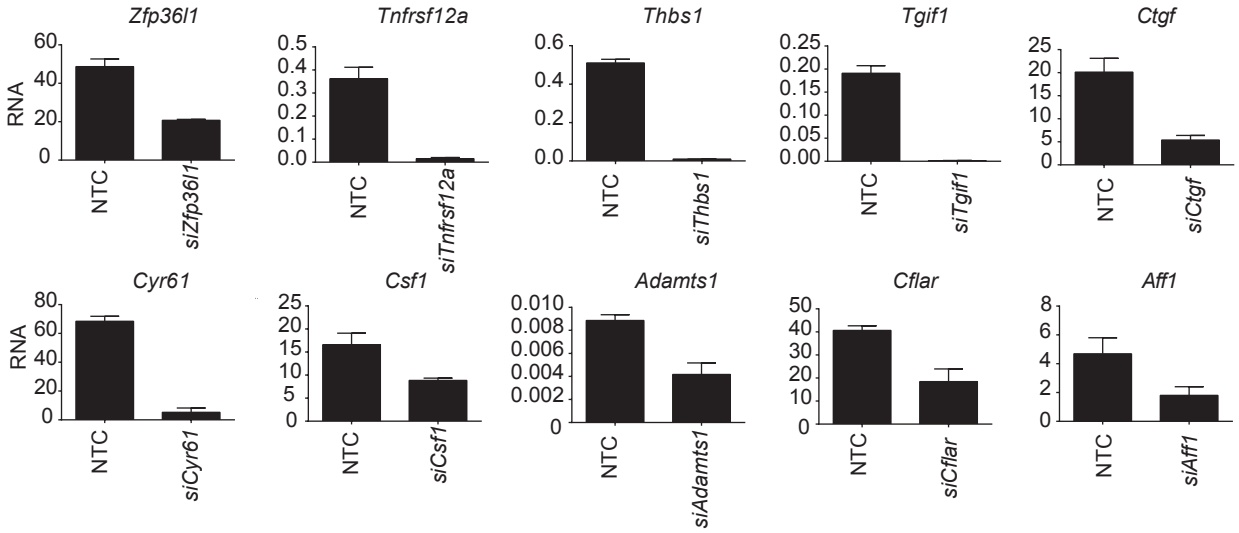
Zfp36l1
Tnfrsf12a
Thbs1
Tgif1
Ctgf
Cyr61
Csf1
Adamts1
Cflar
Aff1
RNA
NTC
siZfp36l1
siTnfrsf12a
siThbs1
siTgif1
siCtgf
siCyr61
siCsf1
siAdamts1
siCflar
siAff1

B

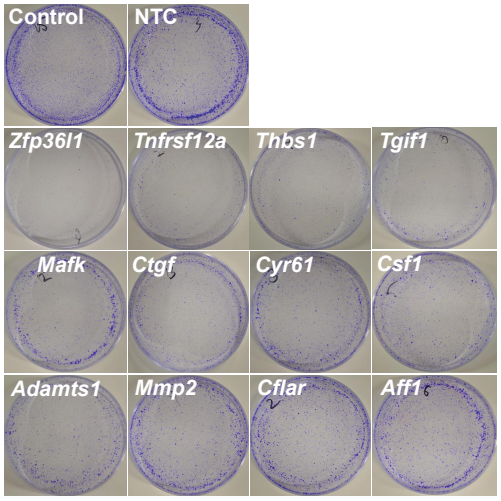
Control
NTC
Zfp36l1
Tnfrsf12a
Thbs1
Tgif1
Mafk
Ctgf
Cyr61
Csf1
Adamts1
Mmp2
Cflar
Aff1

C

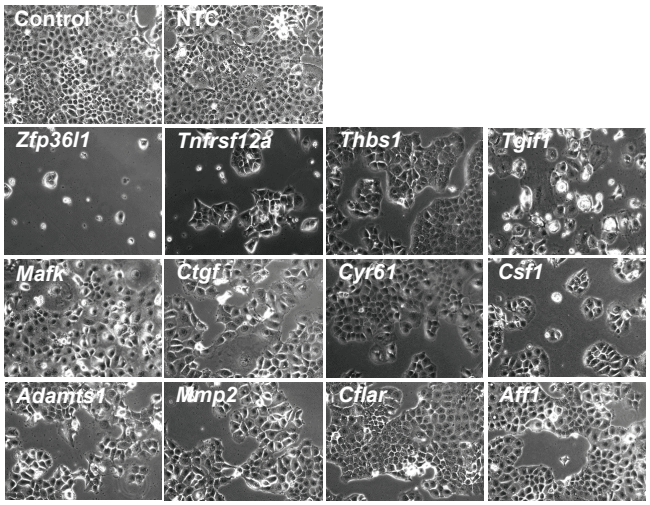
Control
NTC
Zfp36l1
Tnfrsf12a
Thbs1
Tgif1
Mafk
Ctgf
Cyr61
Csf1
Adamts1
Mmp2
Cflar
Aff1

Supplemental Figure S5 **Thakurela & Sahu et al.**

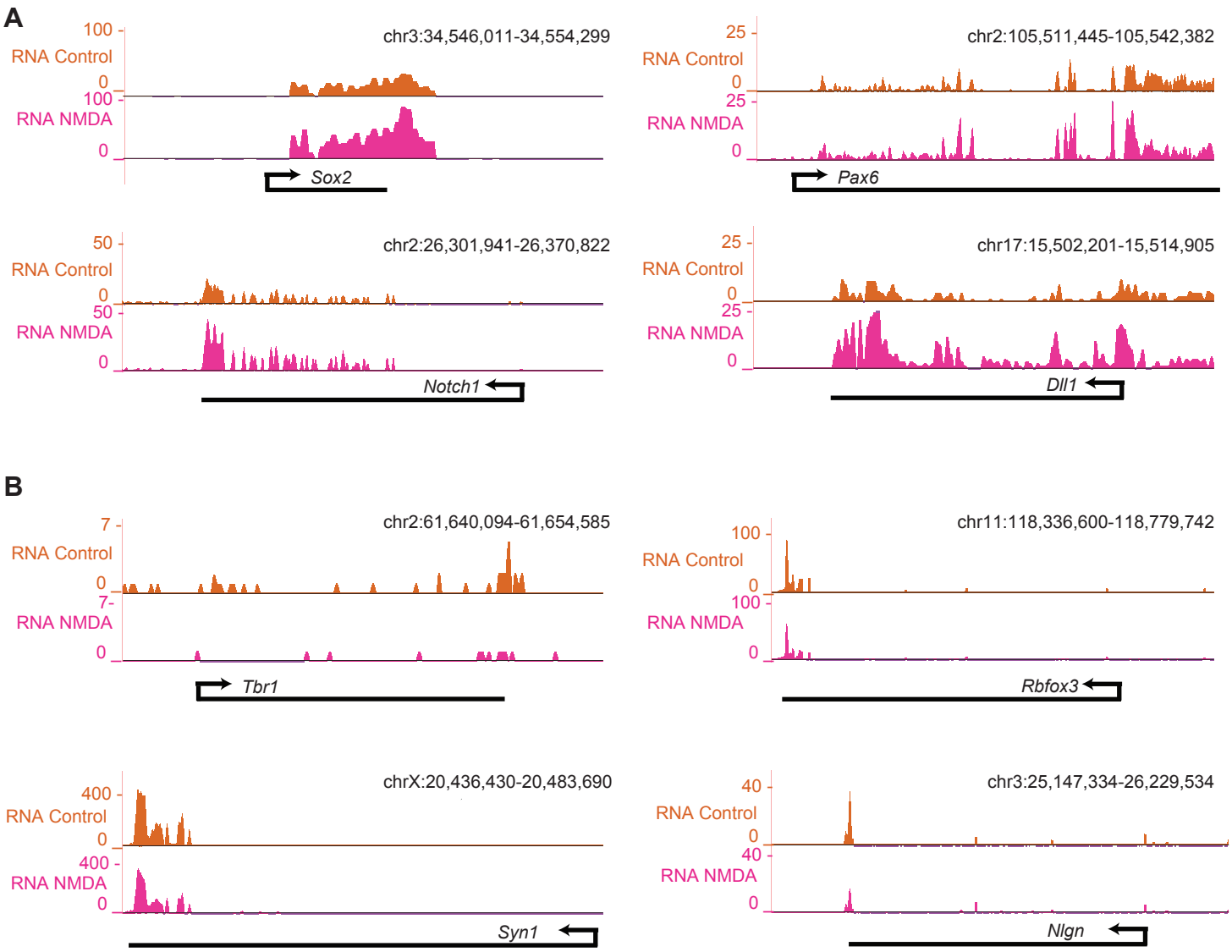

Supplemental Figure S6 **Thakurela & Sahu et al.**

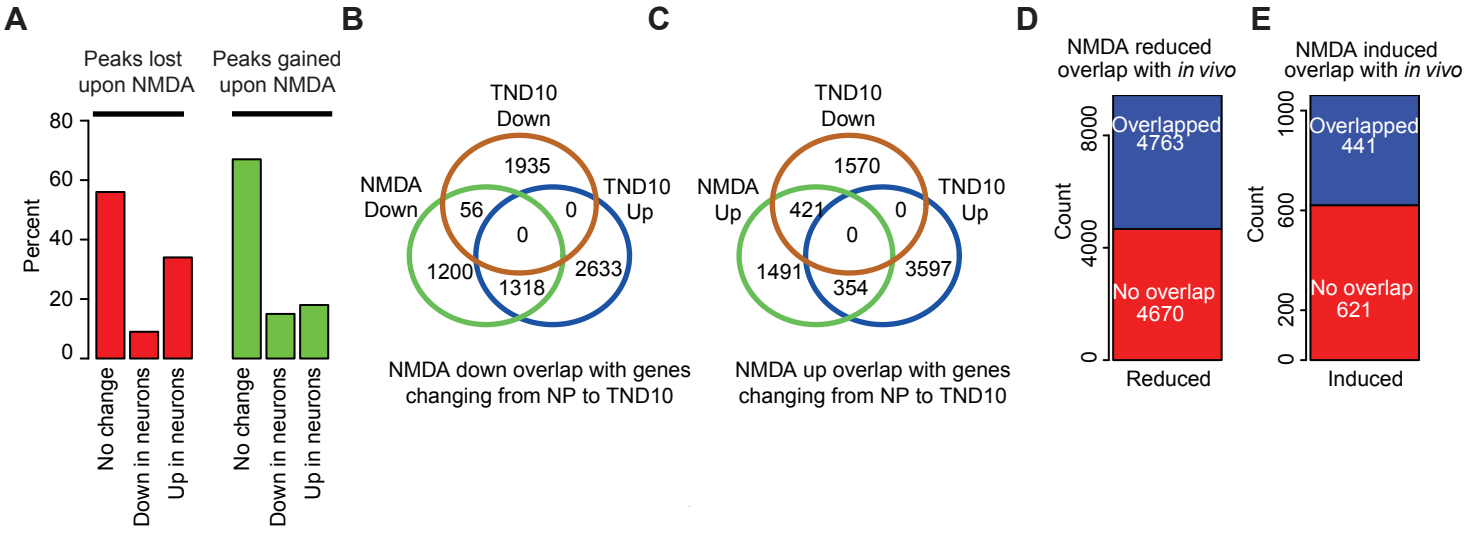

F

NMDA reduced top motifs

Motif	Name	P-value
	RFX	1e-75
	Rfx2	1e-74
	Hoxc9	1e-71
	Pdx1	1e-53
	HOXA9	1e-53
	X-box	1e-51
	Lhx3	1e-45
	Nkx6.1	1e-43
	Isl1	1e-38
	Rfx1	1e-33
	Lhx2	1e-32
	Atf4	1e-31
	Pit1	1e-27
	SCL	1e-26
	Hoxb4	1e-25
	CEBP:AP1	1e-24
	MyoD	1e-22
	Tcf12	1e-22
	Chop	1e-21
	Phox2a	1e-17
	EBF1	1e-17
	Maz	1e-17
	REST-NRSF	1e-17
	EBF	1e-17
	Eomes	1e-17

G

NMDA induced top motifs

Motif	Name	P-value
	NF1	1e-18
	NF1-halfsite	1e-6
	Tlx	1e-5
	Myf5	1e-4
	MyoG	1e-4
	X-box	1e-4
	BMYB	1e-4
	Jun-AP1	1e-4
	TEAD	1e-4
	Rfx1	1e-3
	Tcf12	1e-3
	Fosl2	1e-3
	Sox2	1e-3
	TEAD4	1e-3
	Maz	1e-3
	FOXP1	1e-3
	Ap4	1e-3
	Stat3	1e-3
	Foxo1	1e-3
	Sox6	1e-3
	Rfx2	1e-3
	NFkB	1e-2
	Sox4	1e-2
	p53	1e-2
	SCL	1e-2

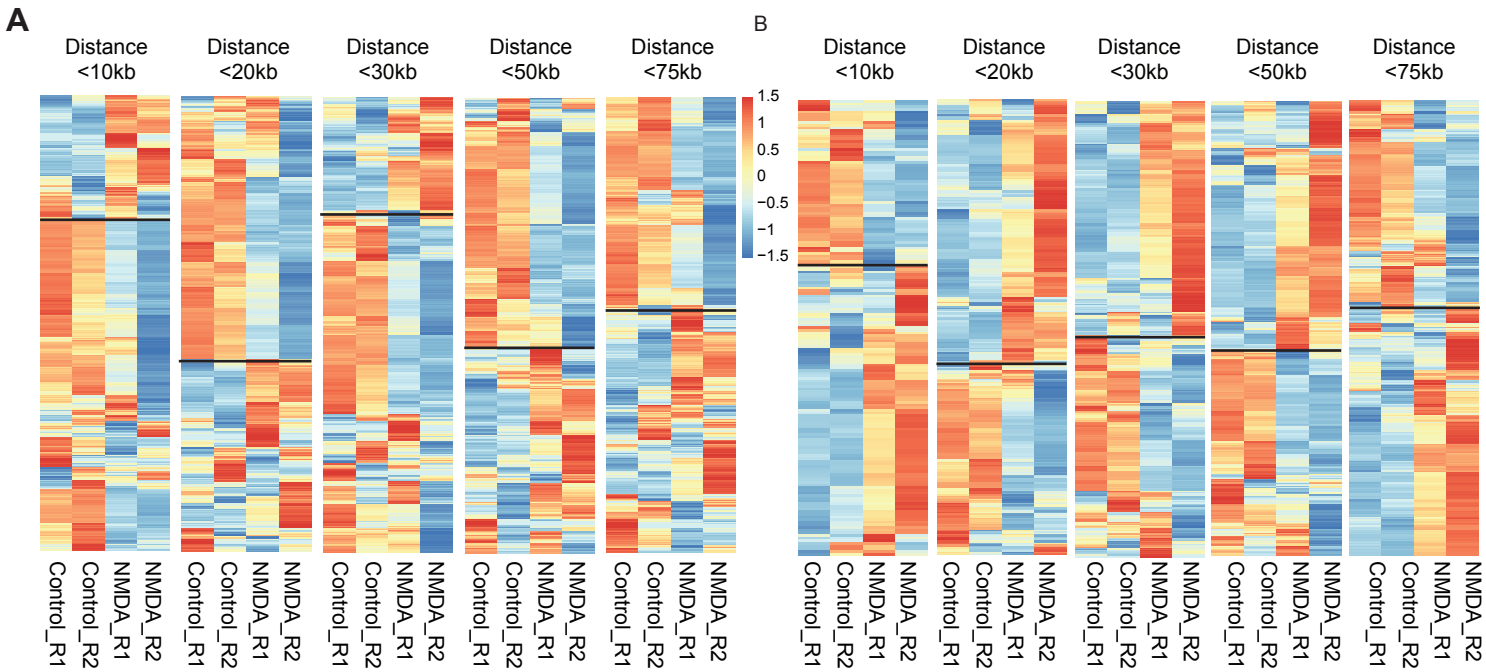
A
B
Distance <10kb
Distance <20kb
Distance <30kb
Distance <50kb
Distance <75kb
1.5
1
0.5
0
−0.5
−1
−1.5
Control_R1
Control_R2
NMDA_R1
NMDA_R2

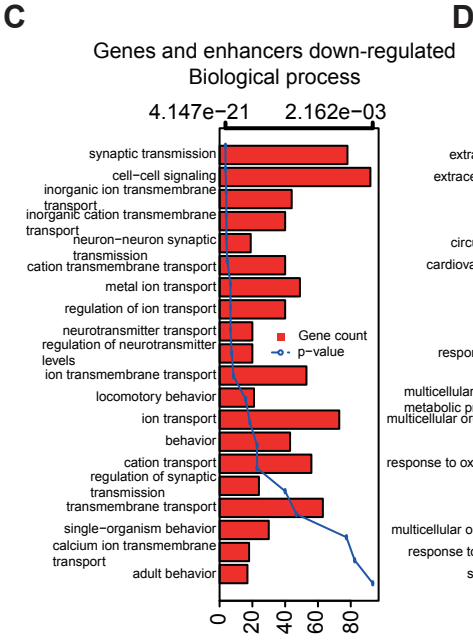
C
Genes and enhancers down-regulated
Biological process
4.147e−21
2.162e−03
synaptic transmission
cell−cell signaling
inorganic ion transmembrane transport
inorganic cation transmembrane transport
neuron−neuron synaptic transmission
cation transmembrane transport
metal ion transport
regulation of ion transport
neurotransmitter transport
regulation of neurotransmitter levels
ion transmembrane transport
locomotory behavior
ion transport
behavior
cation transport
regulation of synaptic transmission
transmembrane transport
single−organism behavior
calcium ion transmembrane transport
adult behavior
Gene count
p−value
0
20
40
60
80

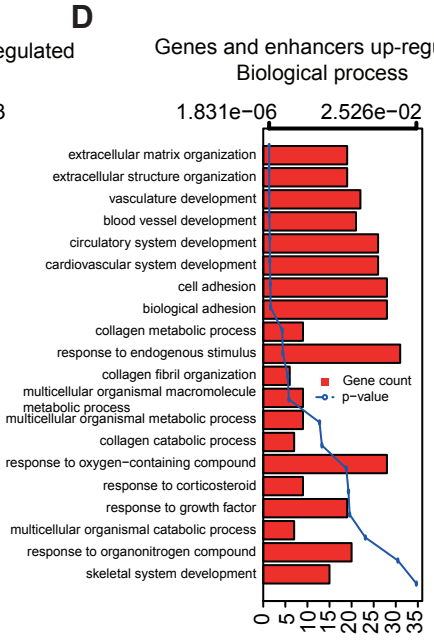
D
Genes and enhancers up-regulated
Biological process
1.831e−06
2.526e−02
extracellular matrix organization
extracellular structure organization
vasculature development
blood vessel development
circulatory system development
cardiovascular system development
cell adhesion
biological adhesion
collagen metabolic process
response to endogenous stimulus
collagen fibril organization
multicellular organismal macromolecule metabolic process
multicellular organismal metabolic process
collagen catabolic process
response to oxygen−containing compound
response to corticosteroid
response to growth factor
multicellular organismal catabolic process
response to organonitrogen compound
skeletal system development
Gene count
p−value
0
5
10
15
20
25
30
35

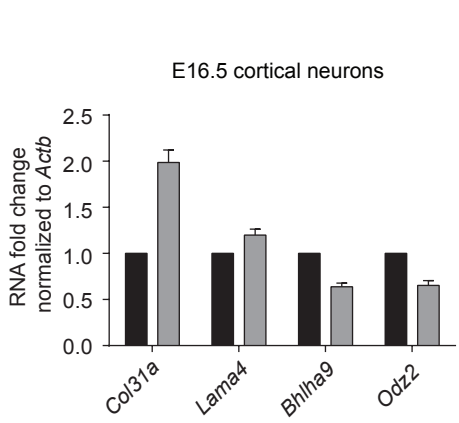
E
E16.5 cortical neurons
RNA fold change normalized to Actb
2.5
2.0
1.5
1.0
0.5
0.0
Col31a
Lama4
Bhlha9
Odz2

A

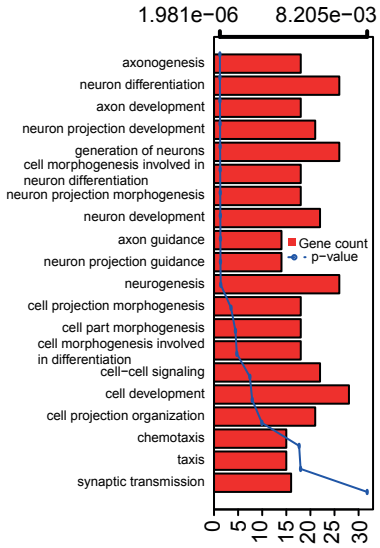
Control only super enhancers
Biological process
1.981e−06
8.205e−03
axonogenesis
neuron differentiation
axon development
neuron projection development
generation of neurons
cell morphogenesis involved in neuron differentiation
neuron projection morphogenesis
neuron development
axon guidance
neuron projection guidance
neurogenesis
cell projection morphogenesis
cell part morphogenesis
cell morphogenesis involved in differentiation
cell−cell signaling
cell development
cell projection organization
chemotaxis
taxis
synaptic transmission
Gene count
p−value
0
5
10
15
20
25
30

B

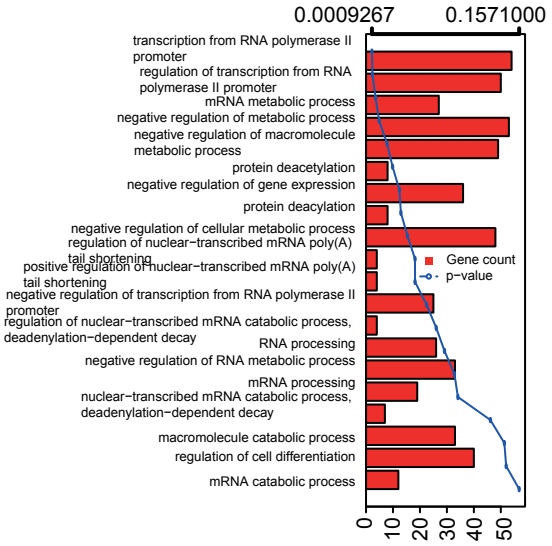
NMDA only super enhancers
Biological process
0.0009267
0.1571000
transcription from RNA polymerase II promoter
regulation of transcription from RNA polymerase II promoter
mRNA metabolic process
negative regulation of metabolic process
negative regulation of macromolecule metabolic process
protein deacetylation
negative regulation of gene expression
protein deacylation
negative regulation of cellular metabolic process
regulation of nuclear−transcribed mRNA poly(A) tail shortening
positive regulation of nuclear−transcribed mRNA poly(A) tail shortening
negative regulation of transcription from RNA polymerase II promoter
regulation of nuclear−transcribed mRNA catabolic process, deadenylation−dependent decay
RNA processing
negative regulation of RNA metabolic process
mRNA processing
nuclear−transcribed mRNA catabolic process, deadenylation−dependent decay
macromolecule catabolic process
regulation of cell differentiation
mRNA catabolic process
Gene count
p−value
0
10
20
30
40
50

Supplemental Figure S9

Thakurela & Sahu et al.

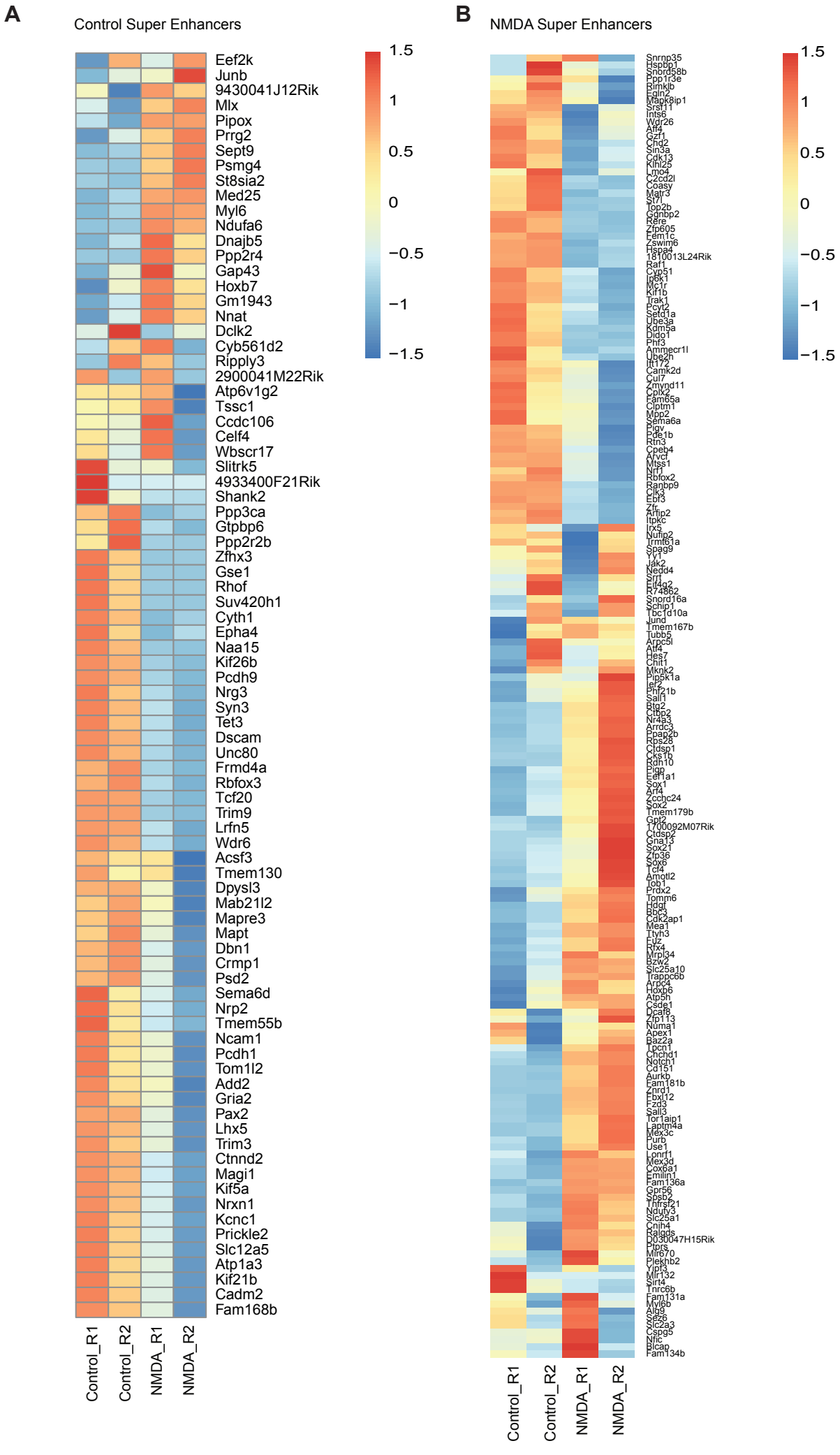

LEGENDS FOR SUPPLEMENTAL FIGURES

Supplemental Figure S1.

(A) Heat map showing correlation of FAIRE-seq replicates. **(B-D)** Scatter plot showing replicate correlation and enrichment distribution of all identified peaks for NP (B), TND1 (C) and TND10 (D). **(E)** Bar plot showing mapping statistics of reads obtained for each FAIRE-seq sample. X-axis represents percentage of alignment. (F) A profile plot showing normalized FAIRE enrichment around TSS of all genes in different stages of neurogenesis. X-axis shows distance from TSS, while y-axis represents library size normalized enrichment. **(G)** Bar plot showing distribution of FAIRE peaks in different genomic locations in NP, TND1 and TND10. **(H)** Bar plot showing feature size normalized distribution of FAIRE peaks in different genomic locations in NP, TND1 and TND10.

Supplemental Figure S2.

(A) Heat map showing the correlation of H3K27ac replicates. **(B-D)** Scatter plot showing the replicate correlation and enrichment distribution of all identified H3K27ac peaks for NP (B), TND1 (C) and TND10 (D). **(E)** Bar plot showing the mapping statistics of H3K27ac ChIP-seq reads obtained for each sample. The x-axis represents the percentage of alignment. **(F)** Bar plot showing the total number of enriched peaks identified in NP, TND1 and TND10. **(G)** Bar plot showing the number of unique enriched peaks identified in NP, TND1 and TND10. **(H)** Box plot showing the distribution of peak width in NP, TND1 and TND10. P-values are calculated using Wilcoxon test. **(I)** A profile plot showing normalized H3K27ac enrichment around the TSS of all genes. The x-axis shows the distance from the TSS; the y-axis represents the library size-normalized enrichment at different stages of neurogenesis. **(J)** Bar plot showing the overlap of all FAIRE peaks with H3K27ac peaks. A peak was considered to be overlapping if the coordinates of FAIRE peaks showed at least 20% overlap with H3K27ac peak. **(K)** Bar plot showing the overlap of unique FAIRE peaks with H3K27ac peaks using the same approach as in J. **(L)** Bar plot showing the overlap of all H3K27ac peaks with FAIRE peaks using 20% overlapping criteria. **(M)** Bar plot showing the overlap of unique

H3K27ac peaks with FAIRE peaks using same criteria as in (L). **(N)** Bar plot showing the number of all H3K27ac peaks that lie within 1 kb from FAIRE peaks. **(O)** Bar plot showing the number of unique H3K27ac peaks that lie within 1 kb from FAIRE peaks. **(P)** Bar plot showing feature size normalized distribution of FAIRE and H3K27ac overlapping peaks in different genomic locations in NP, TND1 and TND10. **(Q)** Box plot showing the expression of adjacent stages for the genes closest to NP, TND1 and TND10 unique H3K27ac sites. Genes were divided into overlapping bins based on the distance of the distal regulatory elements from the TSS. Expression is reported as reads per kilobase of transcript per million mapped reads (RPKM). **(R)** Stacked bar plot showing the overlap of all uniquely identified H3K27ac sites in TND10 with H3K27ac sites from other tissues.

Supplemental Figure S3.

(A) Cell viability assay showing total number of viable cells in control and NMDA treated neurons. **(B)** Representative immunoblots (n=2) showing caspase3 in NMDA induced neuron. β-actin is shown as a loading control. **(C)** Immunofluorescence microscopy for β III Tubulin staining in control and NMDA treated neurons confirming no symptoms of neuronal degeneration. Images were taken at 63X magnification **(D)** mRNA levels for classical activity modulated gene *Npas4* in neuron treated with NMDA or NMDA in presence of NMDAR antagonist DAPV or L-glutamate were measured by qRT-PCRs relative to *Actb* plotted on the y-axis. Error bars represent SEM from independent biological replicates. **(E-F)** mRNA expression kinetics of neuronal activity modulated genes upon various concentrations of NMDA were measured by qRT-PCRs relative to *Actb* and plotted on the y-axis for ES-derived neurons (E) and cortical neurons (F). **(G-H)** Bar plot showing the enrichment of known mouse phenotypes in genes down-regulated (G) and upregulated (H) upon NMDA treatment. The bars reflect the number of genes in each category; the lines represent the multiple tested corrected p-value of the corresponding GO term. **(I)** Volcano plot showing up- and down-regulated lincRNAs upon NDMA treatment in TND10 neurons. The x-axis represents the fold change between control and NDMA in log2; the y-axis shows the adjusted p-value in -log10. **(J)** Heat map showing the expression of the genes nearest to differentially

expressed lincRNAs. **(K)** Density plot showing distance (in kb, log2) of lincRNA from nearest gene TSS. **(L)** Scatter plot displaying changes in expression of lincRNA and corresponding nearest genes. **(M-N)** Bar plots showing enrichment of biological processes in down-(M) and up-regulated (N) genes near down- or up-regulated lincRNAs upon NDMA treatment respectivelly. The bars reflect the number of genes in each category; the lines represent the multiple tested corrected p-value of the corresponding GO term.

Supplemental Figure S4.

(A) mRNA levels for knockdown efficiency of target gene in epithelial cells pre-depleted for two days with specific siRNA against pro-survival genes were measured by qRT-PCR relative to *Actb* and plotted on the y-axis. Error bars represent SEM from independent biological replicates. **(B)** Representative images of colony forming assay performed on epithelial cell after 7 days of siRNA-mediated depletion of pro-survival factors compared to non-targeting control (NTC). **(C)** Representative Bright field images of the cells described in (B).

Supplemental Figure S5.

(A) Representative browser tracks of few progenitor genes showing increase in expression upon NMDA. **(B)** Same as in (A), but showing down-regulation of selected neuronal genes.

Supplemental Figure S6.

(A) Comparison of NMDA modulated H3K27ac peaks with H3K27ac peaks changing between NP and TND10. Peaks that are either losing or gaining two fold enrichment upon NMDA treatment were compared with two fold changing H3K27ac peaks between NP and TND10. A peak was considered to be overlapping, if it was found to be within 1kb distance of peaks modulated during neurogenesis (NP to TND10). **(B)** Venn diagram showing overlap of significantly down-regulated genes upon NMDA with significantly down or up-regulated genes between NP and TND10. **(C)** Same as in (B) but for genes significantly up-regulated upon NMDA. **(D-E)** Stacked bar plot showing the overlap of NMDA-induced (D) or -reduced

(E) peaks with H3K27ac peaks from several embryonic and adult stages taken from E11.5, E14.5, E.17.5, P0, P7, P21, P56 cortex (Nord et al. 2013). **(F-G)** List of top 25 transcription factors motifs identified in NMDA-reduced (F) and NMDA-induced (G) peaks.

Supplemental Figure S7.

(A-B) Heat map showing the expression of genes, binned based on distance (10kb, 20kb, 30kb, 50kb and 75kb) from NMDA-reduced (A) or NMDA-induced distal peaks (B) in control- and NMDA-treated day 10 neurons. **(C-D)** Bar plots showing the enrichment of biological processes in genes that are near to down- and up-regulated distal regulatory regions and their expression reproducibly changed by at least 1.5-fold. The bars reflect the number of genes in each category; the lines represent the multiple tested corrected p-value of the corresponding GO term. ***(E)*** mRNA levels for genes shown in Fig. 7H upon NMDA mediated activation in mouse cortical neurons isolated from E16.5 mouse brain measured by qRT-PCR relative to *Actb* and plotted on the y-axis. Error bars represent SEM from independent biological replicates.

Supplemental Figure S8.

(A) Enrichment of biological process in genes near to non-promoter control only super-enhancers of day 10 neurons. Bars reflect count of gene in each category while line represent multiple tested corrected p-value, displayed as alternate x-axis, of corresponding GO term. **(B)** Same as in (A) but for NMDA unique super-enhancers.

Supplemental Figure S9.

(A-B) Heat maps showing expression of genes near to control (A) and NDMA (B) non-promoter super-enhancers in control and NDMA-treated neurons.